Inorg. Chem. **2007**, *46*, 3116–3122

Crystal Growth and Structural Characterization of the New Ordered Palladates $LnKPdO_3$ (Ln = La, Pr, Nd, Sm–Gd) and the Isostructural, Partially Cu-Substituted Palladate $PrK(Cu_{0.14}Pd_{0.86})O_3$

Samuel J. Mugavero III, Mark D. Smith, and Hans-Conrad zur Loye*

Department of Chemistry and Biochemistry, University of South Carolina, Columbia, South Carolina 29208

Received October 29, 2006

Single crystals of a new series of lanthanide-containing palladates, $LnKPdO_3$ (Ln = La, Pr, Nd, Sm–Gd), and a partially copper-substituted palladate, $PrK(Cu_{0.14}Pd_{0.86})O_3$, were grown from potassium hydroxide fluxes. The compounds are all isostructural and crystallize in the *C*2/*m* space group with lattice parameters ranging from a = 13.4232(8) to 13.0212(2) Å, b = 3.9840(2) to 3.9096(2) Å, c = 7.4424(4) to 7.3209(9) Å, and β = 105.644(2) to 104.427(2)°. The crystal structure contains ordered slabs of LnO_7- and KO_7-capped trigonal prisms arranged in a complex network of face-, edge-, and vertex-shared polyhedra which, in turn, share edges with PdO_4 square planes.

Introduction

The ability to substitute elements for one another in oxides is known for virtually every structure type where, in general, the two most important factors for a given chemical substitution are the size and charge of the constituent cations. In this regard, platinum group metals make excellent substitutes for each other in many structure types because they are very similar in size for a given oxidation state and, furthermore, are able to assume a wide range of oxidation states. An excellent example demonstrating this interchangeability of platinum group metals can be found in the lanthanide-containing double perovskite osmates, ruthenates, and iridates[1] with the general formula $Ln_2MM'O_6$ (Ln = La, Pr, Nd, Sm, Eu; M = Li, Na; M′ = Ru, Os, Ir).[2−6] Similarly, in the 2H-perovskite-related oxides described by the general formula $A_{3n+3m}A'_nB_{3m+n}O_{9m+6n}$,[7−9] a wide variety of platinum group metals, including platinum, rhodium, iridium, and palladium, can substitute on the B site and result in compositions such as Sr_4PtO_6,[10] Sr_4PdO_6, Ca_4PdO_6,[11] and Ca_3MgIrO_6,[12] to name a few.

Other substitutions are more complex and involve the exchange of two divalent cations by one monovalent cation and one trivalent cation. For example, $(NaLa_2)NaPtO_6$ was the first example of a 2H-perovskite-related oxide in which the A-site substitution of an alkaline-earth metal cation by a lanthanide and an alkali-metal cation was accomplished.[13] Since then, several other A-site-substituted 2H-perovskite-related oxides with the general formula $(A_{3-x}Na_x)NaBO_6$ (A = La, Pr, Nd; B = Rh, Pt) have been reported.[14] Similarly, the oxide $Gd_{0.96}Na_{1.04}IrO_4$ is related to Ca_2IrO_4, via the substitution of two Ca cations for one Gd cation and one Na cation. In that series, $Ln_{1-x}Na_{1+x}IrO_4$ (Ln = Gd−Er, Y; x = 0.04−0.25), it is interesting to note that the composition adjusts itself in an attempt to maintain a constant unit-cell

* To whom correspondence should be addressed. E-mail: zurloye@mail.chem.sc.edu.

(1) Mitchell, R. H. *Perovskites Modern and Ancient*; Almaz Press, Inc.: Thunder Bay, ON, 2002.
(2) Mugavero, S. J., III; Smith, M. D.; zur Loye, H.-C. *J. Solid State Chem.* **2005**, *178*, 200.
(3) Mugavero, S. J., III; Puzdrjakova, I. V.; Smith, M. D.; zur Loye, H.-C. *Acta Crystallogr., Sect. E: Struct. Rep. Online* **2005**, *61*, i3.
(4) Gemmill, W. R.; Smith, M. D.; zur Loye, H.-C. *J. Solid State Chem.* **2004**, *177*, 3560.
(5) Gemmill, W. R.; Smith, M. D.; zur Loye, H.-C. *J. Solid State Chem.* **2006**, *179*, 1750.
(6) Gemmill, W. R.; Smith, M. D.; Mozharivsky, Y. A.; Miller, G. J.; zur Loye, H.-C. *Inorg. Chem.* **2005**, *44*, 2639.
(7) Stitzer, K. E.; Darriet, J.; zur Loye, H.-C. *Curr. Opin. Solid State Mater. Sci.* **2001**, *5*, 535.
(8) Perez-Mato, J. M.; Zakhour-Nakhl, M.; Weill, F.; Darriet, J. *J. Mater. Chem.* **1999**, *9*, 2795.
(9) Darriet, J.; Subramanian, M. A. *J. Mater. Chem.* **1995**, *5*, 543.
(10) Randall, J. L.; Katz, L. *Acta Crystallogr., Sect. A* **1959**, *12*, 519.
(11) Wang, Y.; Walker, D.; Chen, B.-H.; Scott, B. A. *J. Alloys Compd.* **1999**, *285*, 98.
(12) Davis, M. J.; Smith, M. D.; zur Loye, H.-C. *Acta Crystallogr.* **2001**, *C57*, 1234.
(13) Davis, M. J.; Smith, M. D.; zur Loye, H.-C. *Inorg. Chem.* **2003**, *42*, 6980.
(14) Macquart, R. B.; Gemmill, W. R.; Davis, M. J.; Smith, M. D.; zur Loye, H.-C. *Inorg. Chem.* **2006**, *45*, 4391.

10.1021/ic062066m CCC: $37.00
Published on Web 03/22/2007

volume (Ln^{3+} (1.00−0.945 Å) and Na^{+} (1.12 Å)).[15] There are, thus, several complex substitutions that can be achieved, including $2Ca^{2+} = Ln^{3+} + Na^{+}$, $2Sr^{2+} = Ln^{3+} + K^{+}$, and $2Ba^{2+} = Ln^{3+} + K^{+}$ for differently sized lanthanides. Traditionally, to achieve such compositional changes, one has relied on solid-state powder synthesis to prepare materials with new compositions, where one or more of the constituent elements from a previously prepared and structurally characterized phase have been substituted.

We have been interested in the discovery of new materials through crystal growth, where we have focused our efforts on studying the reactivity of lanthanide and platinum group metals in alkali-metal hydroxides as a means of growing high-quality single crystals of new oxide materials. Within this group of platinum group metal oxides, the chemistry of new palladates grown from alkali-metal hydroxides remains relatively unexplored. Several years ago, we reported the hydroxide flux synthesis of $CaPd_3O_4$ and $SrPd_3O_4$,[16] and more recently, we succeeded in synthesizing $LuNaPd_6O_8$, a new material structurally related to the APd_3O_4 (A = Ca, Sr) phases,[16−18] from a sodium hydroxide flux. Interestingly, $LuNaPd_6O_8$ represents the first example of an ordered substitution of a lanthanide metal and an alkali metal for an alkaline-earth metal on the A site of a platinum group metal oxide and also the first palladate to contain both a lanthanide and an alkali metal.[19] In an effort to further explore the chemistry of palladium in hydroxide fluxes, we have prepared a new series of ordered, lanthanide- and alkali-metal-containing palladates, $LnKPdO_3$ (Ln = La, Pr, Nd, Sm−Gd), and a partially copper-substituted analogue, $PrK(Cu_{0.14}Pd_{0.86})O_3$, from potassium hydroxide fluxes. For this structural series, we essentially modified the A_2MO_3 (A = Ca, Sr, Ba; M = Cu, Pd)[17,20−29] alkaline-earth metal palladates and cuprates, where we took advantage of the ($2Ba^{2+} = Ln^{3+} + K^{+}$)-type substitution. The crystal growth and structural characterization of the new palladates $LnKPdO_3$ (Ln = La, Pr, Nd, Sm−Gd) and the partially copper-substituted analogue, $PrK(Cu_{0.14}Pd_{0.86})O_3$, are reported herein.

(15) Mugavero, S. J., III; Smith, M. D.; zur Loye, H.-C. *Solid State Sci.* **2007**, in press.
(16) Smallwood, P. L.; Smith, M. D.; zur Loye, H.-C. *J. Cryst. Growth* **2000**, *216*, 299.
(17) Wasel-Nielen, V. H.-D.; Hoppe, R. *Z. Anorg. Allg. Chem.* **1970**, *375*, 209.
(18) Muller-Buschbaum, H. *Z. Anorg. Allg. Chem.* **2005**, *631*, 239.
(19) Mugavero, S. J., III; Smith, M. D.; zur Loye, H.-C. *J. Solid State Chem.* **2006**, *179*, 3586.
(20) Wong-Ng, W.; Davis, K. L.; Roth, R. S. *J. Am. Ceram. Soc.* **1988**, *71*, 64.
(21) Weller, M. T.; Lines, D. R. *J. Solid State Chem.* **1989**, *82*, 21.
(22) Teske, C. L.; Muller-Buschbaum, H. *Z. Anorg. Allg. Chem.* **1969**, *371*, 325.
(23) Teske, C. L.; Muller-Buschbaum, H. *Z. Anorg. Allg. Chem.* **1970**, *379*, 234.
(24) Nagata, Y.; Taniguchi, T.; Tanaka, G.; Satho, M.; Samata, H. *J. Alloys Compd.* **2002**, *346*, 50.
(25) Muller, O.; Roy, R. *Adv. Chem. Ser.* **1971**, *98*, 28.
(26) Lines, D. R.; Weller, M. T.; Currie, D. B.; Ogborne, D. M. *Mater. Res. Bull.* **1991**, *26*, 223.
(27) Laligant, Y.; Le Bail, A.; Ferey, G.; Hervvieu, M.; Raveau, B.; Wilkinson, A.; Cheetham, A. K. *Eur. J. Solid State Inorg. Chem.* **1988**, *25*, 237.
(28) Hjorth, M.; Hyldtoft, J. *Acta Chem. Scand.* **1990**, *44*, 516.
(29) Eremin, N. N.; Leonyuk, L. I.; Urusov, V. S. *J. Solid State Chem.* **2001**, *158*, 162.

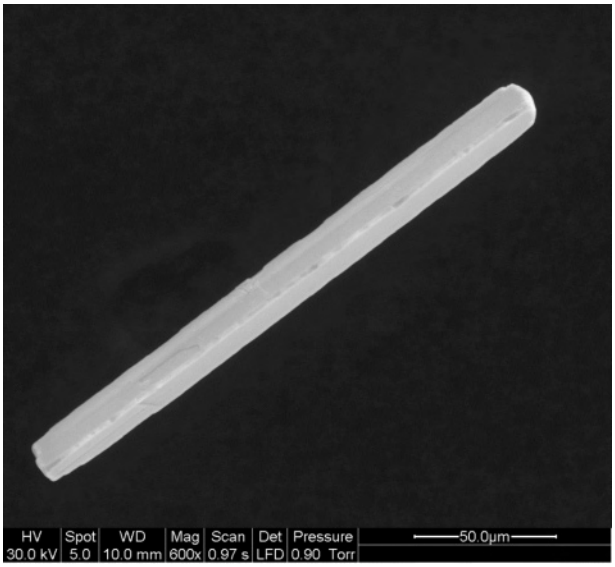

Figure 1. Scanning electron micrograph of a $EuKPdO_3$ single crystal.

Experimental Section

Crystal Growth. Golden-brown, needle-shaped single crystals of $LnKPdO_3$ (Ln = La, Pr, Nd, Sm−Gd) and $PrK(Cu_{0.14}Pd_{0.86})O_3$ were grown from molten potassium hydroxide fluxes. La_2O_3 (Alfa Aesar, 99.9%, 0.5 mmol), Pr_2O_3 (prepared by heating Pr_6O_{11} (Alfa Aesar, 99.9%, 0.5 mmol) in a reducing atmosphere at 1000 °C for several days), Nd_2O_3 (Alfa Aesar, 99.9%, 0.5 mmol), Sm_2O_3 (Alfa Aesar, 99.9%, 0.5 mmol), Eu_2O_3 (Alfa Aesar, 99.9%, 0.5 mmol) or Gd_2O_3 (Alfa Aesar, 99.9%, 0.5 mmol), Pd metal (Engelhard, 99.9%, 1 mmol), and KOH (Fisher, ACS reagent, 15.0 g) were loaded into alumina or silver crucibles and covered. In the case of $PrK(Cu_{0.14}Pd_{0.86})O_3$, CuO (Alfa Aesar, 99.7%, 1 mmol) was utilized as the source of copper. The crucibles were placed into a programmable box furnace and heated to 750 °C in 2 h, held at that temperature for 5 h, and then cooled to 600 °C in 36 h. The reaction was allowed to cool to room temperature by shutting off the furnace. The crystals were removed from the flux matrix by dissolving the flux in water and isolating the crystals by vacuum filtration. Attempts were made to synthesize the analogous $LnK(Cu_xPd_{1-x})O_3$ (Ln = La, Nd, Sm−Gd) phases; however, the reactions failed to yield either single crystals of acceptable quality for single-crystal X-ray diffraction or polycrystalline samples for powder X-ray diffraction.

Scanning Electron Microscopy. Single crystals were analyzed by scanning electron microscopy using an FEI Quanta Scanning electron microscope instrument utilized in the low-vacuum mode. A scanning electron micrograph of a single crystal of $EuKPdO_3$ is shown in Figure 1 and is representative of the crystal morphology observed for both the $LnKPdO_3$ (Ln = La, Pr, Nd, Sm−Gd) series and $PrK(Cu_{0.14}Pd_{0.86})O_3$. Energy-dispersive spectroscopy (EDS) verified the presence of Ln, K, Pd, and O in $LnKPdO_3$ (Ln = La, Pr, Nd, Sm−Gd) and Pr, K, Cu, Pd, and O in $PrK(Cu_{0.14}Pd_{0.86})O_3$ and, within the detection limits of the instrument, confirmed the absence of extraneous elements, such as silver.

Structure Determination. Single crystals of $LnKPdO_3$ (Ln = La, Nd, Pr, Sm−Gd) and $PrK(Cu_{0.14}Pd_{0.86})O_3$ formed as transparent, golden-brown needles. X-ray diffraction intensity data for each were measured at 294(2) K on a Bruker SMART APEX diffractometer (Mo Kα radiation, $\lambda = 0.71073$ Å).[30] The data collections were programmed to provide high redundancy to $2\theta_{max} = 65°$ (62° in the case of Ln = Gd due to small crystal size). Raw area detector

Table 1. Crystallographic Data and Structural Refinement for $LaKPdO_3$, $PrKPdO_3$, $NdKPdO_3$, $SmKPdO_3$, $EuKPdO_3$, and $GdKPdO_3$

	empirical formula		
	$LaKPdO_3$	$PrKPdO_3$	$NdKPdO_3$
fw (g mol^{-1})	332.41	334.41	337.74
space group	*C*2/*m*	*C*2/*m*	*C*2/*m*
unit-cell dimens			
a (Å)	13.4232(8)	13.2620(5)	13.2053(6)
b (Å)	3.9840(2)	3.9576(2)	3.9444(2)
c (Å)	7.4424(4)	7.3865(3)	7.3711(4)
β (deg)	105.644(2)	105.1580(10)	104.970(2)
V (Å^3)	383.26(4)	374.20(3)	370.91(3)
Z	4	4	4
density (calcd) (g cm^{-3})	5.761	5.936	6.048
abs coeff (mm^{-1})	16.602	18.608	19.636
F(000)	584	592	596
cryst size (mm)	0.08 × 0.02 × 0.02	0.08 × 0.04 × 0.02	0.08 × 0.03 × 0.02
θ_{max} (deg)	32.55	32.57	32.54
reflns collected	4344	4041	3117
independent reflns	781	765	758
	[R_{int} = 0.0357]	[R_{int} = 0.0278]	[R_{int} = 0.0344]
goodness-of-fit on F^2	1.100	1.086	1.076
R indices (all data)	R1 = 0.0324	R1 = *0.0165*	R1 = 0.0291
	wR2 = 0.0697	wR2 = 0.0383	wR2 = 0.0566
largest diffraction peak and hole (e Å^{-3})	4.261 and −1.892	0.978 and −1.180	1.884 and −1.686

	empirical formula		
	$SmKPdO_3$	$EuKPdO_3$	$GdKPdO_3$
fw (g mol^{-1})	343.85	345.46	350.75
space group	*C*2/*m*	*C*2/*m*	*C*2/*m*
unit-cell dimens			
a (Å)	13.1015(7)	13.0582(5)	13.0212(2)
b (Å)	3.9281(2)	3.9198(2)	3.9096(2)
c (Å)	7.3400(4)	7.3298(3)	7.3209(4)
β (deg)	104.684(2)	104.5620(10)	104.427(2)
V (Å^3)	365.41(3)	363.13(3)	360.94(3)
Z	4	4	4
density (calcd) (g cm^{-3})	6.250	6.319	6.455
abs coeff (mm^{-1})	21.792	23.030	24.168
F(000)	604	608	612
cryst size (mm)	0.05 × 0.03 × 0.02	0.10 × 0.04 × 0.02	0.06 × 0.02 × 0.01
θ_{max} (deg)	35.52	32.57	31.05
reflns collected	3420	4069	2986
independent reflns	744	743	650
	[R_{int} = 0.0597]	[R_{int} = 0.0303]	[R_{int} = 0.0363]
goodness-of-fit on F^2	1.020	1.148	1.052
R indices (all data)	R1 = 0.0428	R1 = 0.0248	R1 = 0.240
	wR2 = 0.0697	wR2 = 0.0607	wR*2* = 0.0501
largest diffraction peak and hole (e Å^{-3})	3.159 and −2.252	1.958 and −2.974	1.166 and −1.409

data frame integration was performed with SAINT+.[30] The reported unit-cell parameters for each were determined by least-squares refinement of all reflections with $I > 8\sigma(I)$ from each data set. Absorption corrections based on the multiple measurement of equivalent reflections were applied to each dataset with *SADABS*.[30] Direct methods structure solution, difference Fourier calculations, and full-matrix least-squares refinement against F^2 were performed with *SHELXTL*.[31]

$LnKPdO_3$ (Ln = La, Nd, Pr, Sm−Gd) and $PrK(Cu_{0.14}Pd_{0.86})O_3$ are isostructural and crystallize in the space group *C*2/*m* as determined by the pattern of systematic absences in the intensity data and by the successful solution and refinement of the structure. There are six atoms in the asymmetric unit: K1, Ln1, Pd1, and three oxygen atoms O1−O3. All atoms reside on mirror planes (*x*, 0, *z*; Wyckoff site 4*i*). All atoms in each structure were refined with anisotropic displacement parameters. Refinement of the metal site occupancies showed no deviation from unity occupancy in any case, with the exception of $PrK(Cu_{0.14}Pd_{0.86})O_3$. For this compound, refinement of the Pd site occupation factor (sof) yielded sof(Pd1) = 0.955(3). This was ascribed to substitution of Cu onto the Pd site, since Cu was present in the synthesis and the elemental analysis (EDS) indicated the presence of Cu in a 1/4.5 ratio of Cu/Pd. Refinement as a mixed Cu/Pd site resulted in occupancies of 0.863(8) (Pd1)/0.137(8) (Cu1), with the total site occupancy constrained to sum to 1.0. Atomic coordinates and displacement parameters were held equal for the two constituents of the site. Relevant crystallographic information is compiled in Tables 1−6.

Results and Discussion

Single crystals of $LnKPdO_3$ (Ln = La, Pr, Nd, Sm−Gd) and $PrK(Cu_{0.14}Pd_{0.86})O_3$ were grown from molten potassium hydroxide flux reactions. The new materials are structurally related to the A_2MO_3 (A = Ca, Sr, Ba; M = Cu, Pd)[17,20−29]

(30) *SADABS*, versions 6.45, 2.10; Bruker Analytical X-ray Systems, Inc.: Madison, WI, 2003.
(31) Sheldrick, G. M. *SHELXTL*, version 6.14; Bruker Analytical Systems, Inc.: Madison, WI, 2000.

Table 2. Atomic Coordinates and Equivalent Isotropic Displacement Parameters for $LaKPdO_3$, $PrKPdO_3$, $NdKPdO_3$, $SmKPdO_3$, $EuKPdO_3$, and $GdKPdO_3$

	x	*y*	*z*	U_{eq}[a]
		$LaKPdO_3$		
La(1)	0.6503(1)	0	0.0827(1)	0.009(1)
K(1)	0.3574(1)	0	0.4348(2)	0.012(1)
Pd(1)	0.0061(1)	0	0.7746(1)	0.008(1)
O(1)	0.8345(4)	0	0.1358(7)	0.012(1)
O(2)	0.4941(4)	0	0.2030(7)	0.014(1)
O(3)	0.1510(3)	0	0.2862(7)	0.011(1)
		$PrKPdO_3$		
Pr(1)	0.6505(1)	0	0.0810(1)	0.008(1)
K(1)	0.3575(1)	0	0.4356(1)	0.014(1)
Pd(1)	0.0066(1)	0	0.7775(1)	0.007(1)
O(1)	0.8322(2)	0	0.1331(4)	0.011(1)
O(2)	0.4938(2)	0	0.1989(4)	0.013(1)
O(3)	0.1515(2)	0	0.2801(4)	0.010(1)
		$NdKPdO_3$		
Nd(1)	0.6503(1)	0	0.0795(1)	0.008(1)
K(1)	0.3571(1)	0	0.4360(2)	0.014(1)
Pd(1)	0.0066(1)	0	0.7778(1)	0.007(1)
O(1)	0.8318(3)	0	0.1326(6)	0.010(1)
O(2)	0.4937(3)	0	0.1981(6)	0.011(1)
O(3)	0.1516(3)	0	0.2788(6)	0.010(1)
		$SmKPdO_3$		
Sm(1)	0.6504(1)	0	0.0782(1)	0.009(1)
K(1)	0.3568(2)	0	0.4357(3)	0.016(1)
Pd(1)	0.0068(1)	0	0.7791(1)	0.008(1)
O(1)	0.8305(5)	0	0.1299(9)	0.011(1)
O(2)	0.4943(5)	0	0.1960(10)	0.015(1)
O(3)	0.1525(5)	0	0.2761(9)	0.012(1)
		$EuKPdO_3$		
Eu(1)	0.6504(1)	0	0.0774(1)	0.009(1)
K(1)	0.3565(1)	0	0.4361(2)	0.015(1)
Pd(1)	0.0070(1)	0	0.7792(1)	0.008(1)
O(1)	0.8305(3)	0	0.1310(6)	0.012(1)
O(2)	0.4938(3)	0	0.1946(6)	0.014(1)
O(3)	0.1523(3)	0	0.2740(6)	0.012(1)
		$GdKPdO_3$		
Gd(1)	0.6502(1)	0	0.0763(1)	0.009(1)
K(1)	0.3564(1)	0	0.4371(2)	0.015(1)
Pd(1)	0.0700(1)	0	0.7792(1)	0.008(1)
O(1)	0.8295(4)	0	0.1309(7)	0.013(1)
O(2)	0.4938(4)	0	0.1937(8)	0.013(1)
O(3)	0.1528(3)	0	0.2725(7)	0.010(1)

[a] U_{eq} is defined as one-third of the trace of the orthogonalized U_{ij} tensor.

alkaline-earth metal palladates and cuprates, and the crystal structure of $LnKPdO_3$ is shown in Figure 2. The structure contains ordered slabs of Ln^{3+} and K^+ in a seven-coordinate environment and Pd^{2+} atoms in a square-planar coordination environment. In each slab, there are six LnO_7- or KO_7-capped trigonal prisms, with four centrally located and one located at each edge of the unit cell along the *x* direction of the slab. The four centrally located LnO_7- or KO_7-capped trigonal prisms edge-share with each other and corner-share with the apical oxygen of the cap of the additional LnO_7- or KO_7-capped trigonal prisms near the edge of the cell along the *x* direction. The LnO_7- and KO_7-capped trigonal prisms further connect via the sharing of one triangular face along the *z* direction to form infinite chains of $LnO_7-KO_7-LnO_7$ polyhedra. Figure 3 shows a comparison of the chains running along the *z* direction for both the (a) $LnKPdO_3$ structure and the (b) Ba_2PdO_3 structure. The square-planar coordination environment of the Pd atoms is slightly distorted from ideal in that the square planes are made up of two equivalent and two nonequivalent Pd−O bond lengths (Table 3). The PdO_4 square planes are situated perpendicular to the

Table 3. Selected Interatomic Distances (Å) for $LaKPdO_3$, $PrKPdO_3$, $NdKPdO_3$, $SmKPdO_3$, $EuKPdO_3$, and $GdKPdO_3$

$LaKPdO_3$		$PrKPdO_3$	
Pd(1)−O(1)	2.062(5)	Pd(1)−O(1)	2.065(3)
Pd(1)−O(2) × 2	1.9990(5)	Pd(1)−O(2) × 2	1.9866(3)
Pd(1)−O(3)	2.034(4)	Pd(1)−O(3)	2.028(3)
La(1)−O(1)	2.397(5)	Pr(1)−O(1)	2.339(3)
La(1)−O(1) × 2	2.614(3)	Pr(1)−O(1) × 2	2.5800(18)
La(1)−O(2)	2.461(5)	Pr(1)−O(2)	2.422(3)
La(1)−O(2)	2.492(5)	Pr(1)−O(2)	2.455(3)
La(1)−O(3) × 2	2.501(3)	Pr(1)−O(3) × 2	2.4631(16)
K(1)−O(1) × 2	2.940(4)	K(1)−O(1) × 2	2.938(2)
K(1)−O(2)	2.837(5)	K(1)−O(2)	2.824(3)
K(1)−O(2)	2.888(5)	K(1)−O(2)	2.897(3)
K(1)−O(3)	2.692(5)	K(1)−O(3)	2.673(3)
K(1)−O(3) × 2	2.901(4)	K(1)−O(3) × 2	2.911(2)
$NdKPdO_3$		$SmKPdO_3$	
Pd(1)−O(1)	2.064(4)	Pd(1)−O(1)	2.065(6)
Pd(1)−O(2) × 2	1.9803(4)	Pd(1)−O(2) × 2	1.9730(7)
Pd(1)−O(3)	2.021(4)	Pd(1)−O(3)	2.023(6)
Nd(1)−O(1)	2.327(4)	Sm(1)−O(1)	2.293(6)
Nd(1)−O(1) × 2	2.565(3)	Sm(1)−O(1) × 2	2.539(4)
Nd(1)−O(2)	2.407(4)	Sm(1)−O(2)	2.390(7)
Nd(1)−O(2)	2.444(4)	Sm(1)−O(2)	2.414(7)
Nd(1)−O(3) × 2	2.457(3)	Sm(1)−O(3) × 2	2.439(4)
K(1)−O(1) × 2	2.936(3)	K(1)−O(1) × 2	2.936(5)
K(1)−O(2)	2.823(4)	K(1)−O(2)	2.819(8)
K(1)−O(2)	2.900(5)	K(1)−O(2)	2.905(7)
K(1)−O(3)	2.661(5)	K(1)−O(3)	2.636(6)
K(1)−O(3) × 2	2.906(3)	K(1)−O(3) × 2	2.912(5)
$EuKPdO_3$		$GdKPdO_3$	
Pd(1)−O(1)	2.057(4)	Pd(1)−O(1)	2.066(5)
Pd(1)−O(2) × 2	1.9695(4)	Pd(1)−O(2) × 2	1.9651(6)
Pd(1)−O(3)	2.018(4)	Pd(1)−O(3)	2.020(4)
Eu(1)−O(1)	2.285(4)	Gd(1)−O(1)	2.268(5)
Eu(1)−O(1) × 2	2.535(3)	Gd(1)−O(1) × 2	2.528(3)
Eu(1)−O(2)	2.373(4)	Gd(1)−O(2)	2.362(5)
Eu(1)−O(2)	2.410(4)	Gd(1)−O(2)	2.400(5)
Eu(1)−O(3) × 2	2.429(2)	Gd(1)−O(3) × 2	2.421(3)
K(1)−O(1) × 2	2.929(3)	K(1)−O(1) × 2	2.929(4)
K(1)−O(2)	2.818(4)	K(1)−O(2)	2.822(5)
K(1)−O(2)	2.913(4)	K(1)−O(2)	2.913(6)
K(1)−O(3)	2.632(4)	K(1)−O(3)	2.624(5)
K(1)−O(3) × 2	2.914(3)	K(1)−O(3) × 2	2.913(4)

Table 4. Crystallographic Data and Structural Refinement for $PrK(Cu_{0.14(1)}Pd_{0.86(1)})O_3$

empirical formula	$PrK(Cu_{0.14(1)}Pd_{0.86(1)})O_3$
fw (g mol^{-1})	328.52
space group	*C*2/*m*
unit-cell dimens	
a (Å)	13.2512(7)
b (Å)	3.9488(2)
c (Å)	7.3773(4)
β (deg)	105.122(2)
V ($Å^3$)	372.66(3)
Z	4
density (calcd) (g cm^{-3})	5.855
abs coeff (mm^{-1})	18.806
F(000)	583
cryst size (mm)	0.08 × 0.03 × 0.02
θ_{max} (deg)	32.56
reflns collected	3899
independent reflns	759 [R_{int} = 0.0384]
goodness-of-fit on F^2	1.083
R indices (all data)	R1 = 0.0306, wR2 = 0.0682
largest diffraction peak and hole (e $Å^{-3}$)	2.044 and −1.661

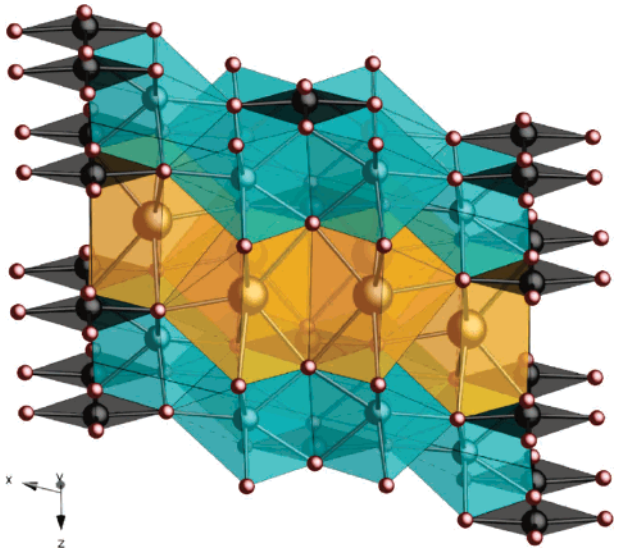

Figure 2. Structural representation of $LnKPdO_3$ with LnO_7-capped trigonal prisms shown in teal, KO_7-capped trigonal prisms shown in orange, and PdO_4 square planes shown in black. O atoms are represented as red spheres.

Table 5. Atomic Coordinates and Equivalent Isotropic Displacement Parameters for $PrK(Cu_{0.14(1)}Pd_{0.86(1)})O_3$

	x	*y*	*z*	U_{eq}[a]
Pr(1)	0.6505(1)	0	0.0810(1)	0.009(1)
K(1)	0.3572(1)	0	0.4356(2)	0.016(1)
Cu(1)/Pd(1)	0.0067(1)	0	0.7782(1)	0.008(1)
O(1)	0.8329(4)	0	0.1323(6)	0.012(1)
O(2)	0.4936(4)	0	0.2003(7)	0.014(1)
O(3)	0.1512(4)	0	0.2808(7)	0.012(1)

[a] U_{eq} is defined as one-third of the trace of the orthogonalized U_{ij} tensor.

z direction and occupy the space created in the middle of four of the LnO_7- and KO_7-capped trigonal prisms. The complex connectivity of the capped trigonal prisms leads to an evenly spaced distribution of PdO_4 square planes along the *x* and *y* directions, with the distance between Pd atoms equal to the *a* and *b* lattice parameters, respectively.

Table 6. Selected Interatomic Distances (Å) for $PrK(Cu_{0.14(1)}Pd_{0.86(1)})O_3$

Cu(1)/Pd(1)−O(1)	2.054(5)
Cu(1)/Pd(1)−O(2) × 2	1.9809(4)
Cu(1)/Pd(1)−O(3)	2.023(5)
Pr(1)−O(1)	2.347(5)
Pr(1)−O(1) × 2	2.570(3)
Pr(1)−O(2)	2.426(5)
Pr(1)−O(2)	2.460(5)
Pr(1)−O(3) × 2	2.463(3)
K(1)−O(1) × 2	2.938(3)
K(1)−O(2)	2.814(5)
K(1)−O(2)	2.890(5)
K(1)−O(3)	2.670(5)
K(1)−O(3) × 2	2.900(4)

However, because the Ln^{3+} cation and the K^+ cation are of unequal size, the Pd atoms along the *z* direction are unevenly spaced. The Pd−Pd distances vary as a function of the size of the lanthanide and, as the size of the lanthanide decreases, the distance between the Pd atoms decreases as well. Thus, the decrease in the lattice parameters (Table 1) is controlled solely by the size of the lanthanide cation.

$LnKPdO_3$ (Ln = La, Pr, Nd, Sm−Gd) and $PrK(Cu_{0.14}Pd_{0.86})O_3$ differ from the A_2MO_3 (A = Sr, Ba) phases[17,25,27] in that, in place of two Sr^{2+} or Ba^{2+} cations, an ordered, 1:1 arrangement of Ln^{3+} and K^+ cations is observed. The overall charge on the A site remains 4+ but is maintained by one Ln^{3+} atom and one K^+ atom. The general formula AA′MO_3, where A and A′ are two divalent cations or the combination of one trivalent cation and one monovalent cation, can be utilized to describe the stoichiometry. As a result of this ordered cation substitution, the *c* parameter effectively doubles, a reduction in symmetry is observed, and the space group changes from orthorhombic (*Immm*) to monoclinic (*C*2/*m*). The reduction in symmetry and ordering can be attributed to the significant size and charge difference of the Ln^{3+} and K^+ cations, where the Ln^{3+} cation (1.06−1.00 Å) is much smaller than K^+ (1.46 Å)[32] and most likely the dominant force of cation ordering.

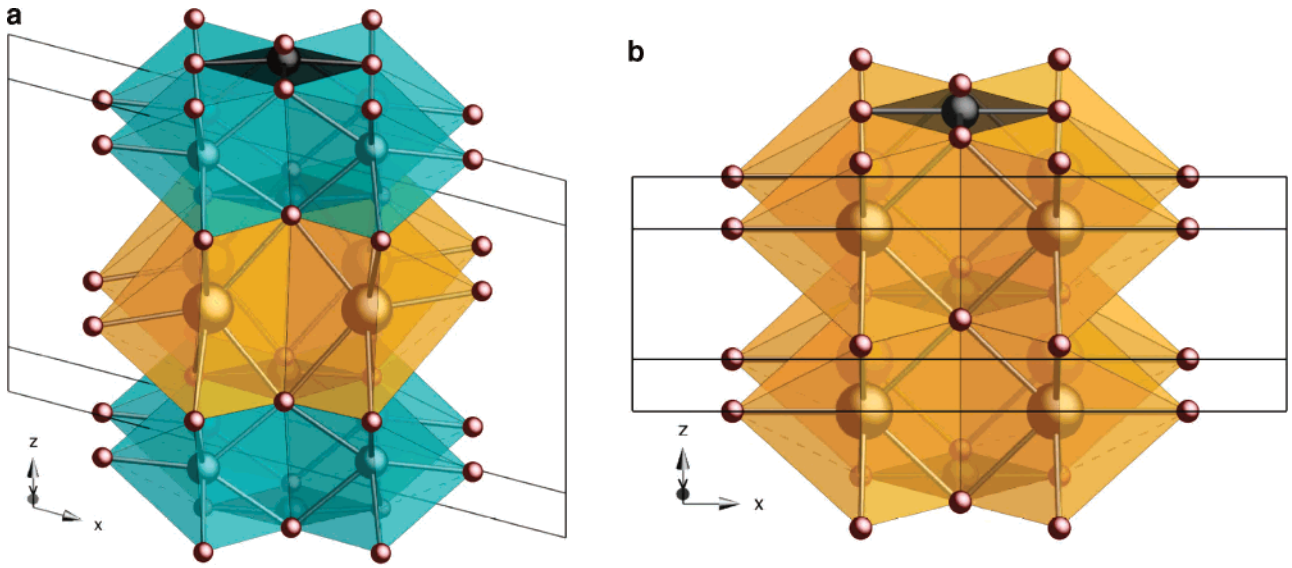

Figure 3. (a) Face-shared chains along the *z* direction of LnO_7−KO_7−LnO_7-capped trigonal prisms. (b) For comparison, BaO_7−BaO_7 face-shared-capped trigonal prisms of the structurally related phase Ba_2PdO_3.

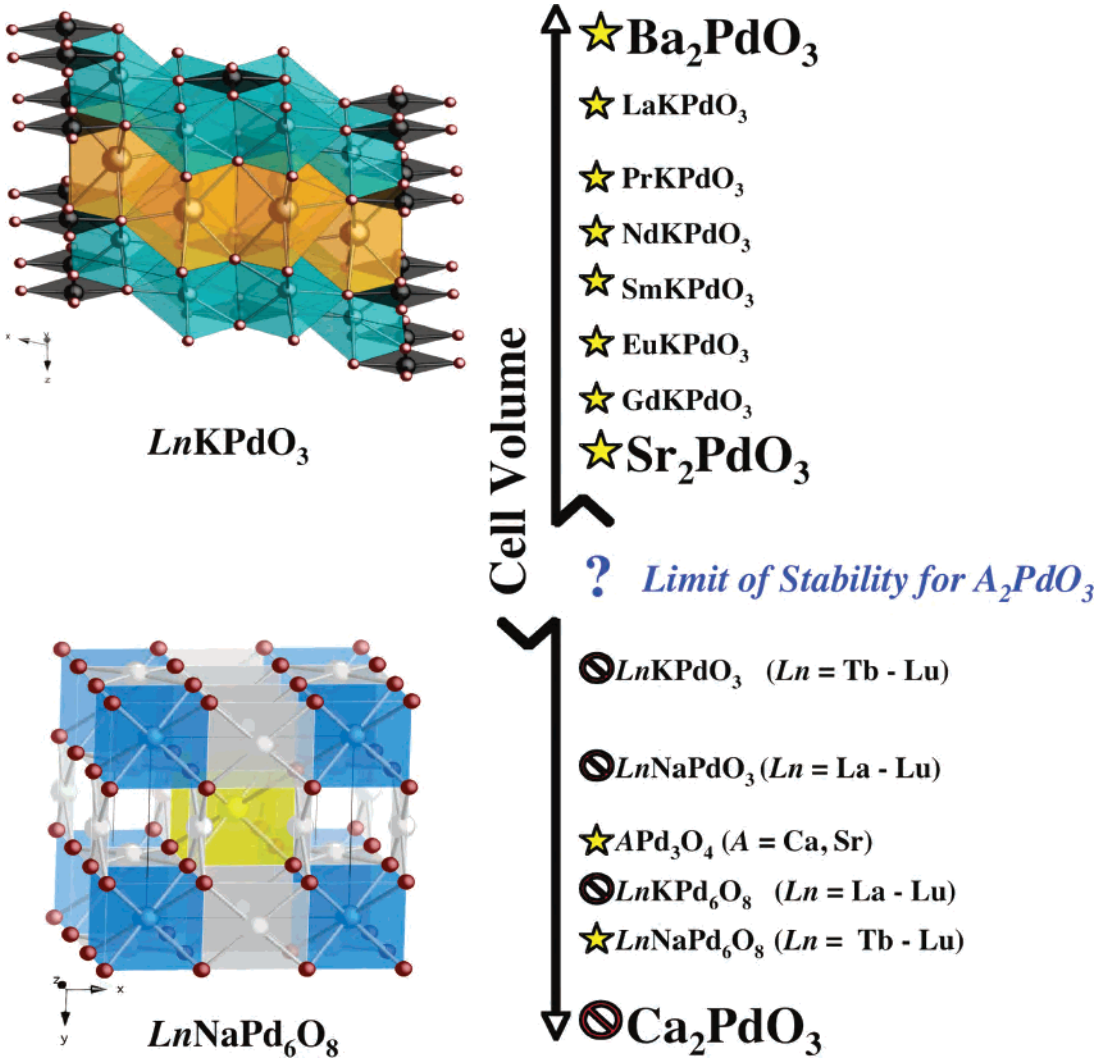

Figure 4. Cartoon displaying the decrease in cell volume in the A_2PdO_3-type structures as one Ln^{3+} cation and one K^+ cation are substituted for two Ba^{2+} cations, leading ultimately to Sr_2PdO_3, situated slightly above the apparent limit of stability. On the basis of cell volume, phases that have been synthesized are indicated by a star (☆) and phases that have not been synthesized and should not form are indicated by a "no symbol" (⊖).

When analyzing the structural relationship between the A_2PdO_3 (A = Sr, Ba)[17,25,27] and the $LnKPdO_3$ (Ln = La, Pr, Nd, Sm−Gd) compositions, we can consider the existence of a structure stability limit based on the size of the A cations. The Ba_2PdO_3 phase roughly represents the upper limit of stability, since Ba is the largest alkaline-earth metal, and Sr_2PdO_3 roughly represents the lower limit, since the A_2PdO_3-type structure does not form for Ca^{2+}, for which the cubic $CaPd_3O_4$ phase is observed.[16,17,25] The ionic radii of Ba^{2+} and Sr^{2+} cations in a seven-coordinate environment are 1.38 and 1.21 Å, respectively; therefore, the range of the average ionic radii on the A site of the $LnKPdO_3$ (1.26−1.23 Å) phases ideally falls between 1.38 and 1.21 Å.[32] In the $LnKPdO_3$ phases, the two divalent A cations have been replaced by one trivalent A cation and one monovalent A′ cation, giving the general formula AA′PdO_3. The primary structural difference between the A_2PdO_3 and AA′PdO_3 structures is the effective doubling of the *c* parameter; thus, we can roughly estimate the cell volume of A_2PdO_3 (A = Sr, Ba) in the monoclinic AA′PdO_3 structure from the lattice parameters if we double the *c* parameter in the orthorhombic cell. The estimated cell volumes of A_2PdO_3 (A = Sr, Ba) in *C*2/*m* and the cell volumes of the AA′PdO_3 phases as determined crystallographically are shown in Table 7. Unlike the $Ln_{1-x}Na_{1+x}IrO_4$ (Ln = Gd−Er, Y) structure, where a relatively constant cell volume is maintained by adjusting the sodium content to counter the effect that the size of the smaller lanthanide cations has on the structure, the $LnKPdO_3$ structure appears to accommodate a range of cell volumes while maintaining a 1:1 order of the Ln^{3+} and K^+ cations. The cartoon in Figure 4 offers a visual representation of the

Table 7. Cell Volumes of the A_2PdO_3-type Oxides[a]

composition	cell volume (Å^3)
Ba_2PdO_3	417.47(2)
$LaKPdO_3$	383.26(4)
$PrKPdO_3$	374.20(3)
$NdKPdO_3$	370.91(4)
$SmKPdO_3$	365.41(3)
$EuKPdO_3$	363.13(3)
$GdKPdO_3$	360.94(3)
Sr_2PdO_3	359.96(1)

[a] The cell volumes for Ba_2PdO_3 and Sr_2PdO_3 were estimated by assuming that these phases could crystallize in the monoclinic $LnKPdO_3$ structure.

(32) Shannon, R. D. *Acta Crystallogr., Sect. A* **1976**, *32*, 751.

change in cell volume as a result of the decrease in the A- and A′-cation size, where the limit of stability for A_2PdO_3-type compounds appears to exist just slightly below Sr_2PdO_3. As a consequence of this structural limitation, the analogous $LnKPdO_3$ (Ln = Tb−Lu) and $LnNaPdO_3$ (Ln = La−Lu) should not be stable because the cell volume in these compounds falls below the apparent limit. Interestingly, if one substitutes a smaller lanthanide (Tb−Lu) in place of a larger lanthanide (La−Gd) while simultaneously substituting sodium for potassium, the structural analogues to $LuNaPd_6O_8$, $LnNaPd_6O_8$ (Ln = Tb−Yb, Y) (Figure 4, bottom left), phases result.[19,33] However, replacing the sodium by potassium in anticipation of synthesizing the analogous $LnKPd_6O_8$ (Ln = Tb−Lu, Y) phases is apparently unsuccessful because the cubic structure cannot accommodate the size difference that exists between the small lanthanide cations and the much larger K^+ cation in an eight-coordinate environment.

The partial substitution of copper in place of palladium in the $PrK(Cu_{0.14}Pd_{0.86})O_3$ phase is interesting in that only a small percentage of copper ended up in the structure. We postulated that because of the existence of isostructural A_2CuO_3 (A = Ca, Sr, Ba) phases[20−23,26,28,29] and the copper palladates, $Sr_2(Pd_{1-x}Cu_x)O_3$ ($0 \le x \le 1$),[24] perhaps an ordered $LnKCu_{0.5}Pd_{0.5}O_3$ structure would result. However, because copper is readily dissolved in hydroxide fluxes and forms very stable phases in the presence of lanthanides,[34,35] it appears that there may be a kinetic competition for the copper and thus only a small percentage of copper was substituted into the $PrK(Cu_{0.14}Pd_{0.86})O_3$ structure.

(33) Mugavero, S. J., III; Smith, M. D.; zur Loye, H.-C., manuscript in preparation.

Conclusion

Single crystals of a new series of ordered, rare-earth palladates, $LnKPdO_3$ (Ln = La, Pr, Nd, Sm−Gd), and a copper-substituted palladate, $PrK(Cu_{0.14}Pd_{0.86})O_3$, have been synthesized from potassium hydroxide fluxes. The materials are all isostructural and contain ordered slabs of LnO_7- and KO_7-capped trigonal prisms and isolated PdO_4 square planes. Work is currently underway to further explore the synthesis of novel palladates and examine structural relationships that may exist within this regime.

Acknowledgment. Financial support from the Department of Energy through Grant No. DE-FG02-04ER46122 and the National Science Foundation through Grant No. DMR:0450103 is gratefully acknowledged.

Supporting Information Available: Seven CIF files. This material is available free of charge via the Internet at http://pubs.acs.org. Further details of the crystal structure investigations can be obtained from the Fachinformationszentrum Karlsruhe, 76344 Eggenstein-Leopoldshafen, Germany (fax, +49-7247-808-666; e-mail, cyrstdata@fiz-karlsruhe.de), on quoting the depository numbers CSD-417102-417108.

IC062066M

(34) Luce, J. L.; Stacy, A. M. *Chem. Mater.* **1997**, *9*, 1508.
(35) Keller, S. W.; Carlson, V. A.; Sandford, D.; Stenzl, F.; Stacy, A. M.; Kwei, G. H.; Alario-Franco, M. *J. Am. Chem. Soc.* **1994**, *116*, 8070.